Ma GH, Zhang ML, Li XM *et al.* Image smoothing based on image decomposition and sparse high frequency gradient. JOURNAL OF COMPUTER SCIENCE AND TECHNOLOGY 33(3): 502–510 May 2018. DOI 10.1007/s11390-018-1834-3

Image Smoothing Based on Image Decomposition and Sparse High Frequency Gradient

Guang-Hao Ma[1], Ming-Li Zhang[2], Xue-Mei Li[3,*], and Cai-Ming Zhang[2,3,4]

[1] *School of Computer Science and Technology, Shandong University, Jinan 250101, China*

[2] *Shandong Co-Innovation Center of Future Intelligent Computing, Yantai 264025, China*

[3] *School of Software, Shandong University, Jinan 250101, China*

[4] *Digital Media Research Institute, Shandong University of Finance and Economics, Jinan 250061, China*

E-mail: {mgh0314, zhangmellie}@gmail.com; {xmli, czhang}@sdu.edu.cn

Received January 5, 2018; revised March 30, 2018.

Abstract Image smoothing is a crucial image processing topic and has wide applications. For images with rich texture, most of the existing image smoothing methods are difficult to obtain significant texture removal performance because texture containing obvious edges and large gradient changes is easy to be preserved as the main edges. In this paper, we propose a novel framework (DSHFG) for image smoothing combined with the constraint of sparse high frequency gradient for texture images. First, we decompose the image into two components: a smooth component (constant component) and a non-smooth (high frequency) component. Second, we remove the non-smooth component containing high frequency gradient and smooth the other component combining with the constraint of sparse high frequency gradient. Experimental results demonstrate the proposed method is more competitive on efficiently texture removing than the state-of-the-art methods. What is more, our approach has a variety of applications including edge detection, detail magnification, image abstraction, and image composition.

Keywords image smoothing, texture removal, image decomposition

1 Introduction

Image smoothing is always a very important problem in image processing and has wide applications. Natural images usually contain clear edges and rich details, such as texture. The human visual system can easily understand the natural image and does not have to consider the texture, because the human perception is sensitive to the principal structure. Image smoothing studies are expected to achieve the same goals: 1) preserving the global features of the image, including the principal structure and edge, and 2) removing some of the details of the image, such as noise and texture.

Over the past few decades, image smoothing has attracted much research attention. Rudin *et al.*[1] proposed the well-known total variation (TV) regular term with L_1 norm gradient magnitude in 1992. It is widely applied in image denoising, because it can preserve large-scale edges and remove noise. Tomas and Manduchi[2] proposed a bilateral filter (BLF), where the candidate pixel in the image is set as a weighted average mean of its neighborhood. It is a simple, local and non-iterative method. Farbman *et al.*[3] proposed an alternative edge-preserving smoothing operator, based on the weighted least squares (WLS) optimization framework in 2008, which involves an L_2 norm. WLS is particularly well suited for progressive coarsening of images and for edge-preserving multi-scale detail extraction. Subr *et al.*[4] proposed a new model for detail that inherently captures oscillations in 2009, a key pro-

Regular Paper

Special Section of CVM 2018

This work was supported by the National Natural Science Foundation of China under Grant Nos. 61373078, 61572292, 61602277, and 61332015, the Key Project of National Natural Science Foundation of China Joint Fund with Zhejiang Integration of Informatization and Industrialization under Grant No. U1609218, and the Natural Science Foundation of Shandong Province of China under Grant No. ZR2016FQ12.

*Corresponding Author

perty that distinguishes texture from individual edges. Cho and Lee[5] presented a fast deblurring method that produces a deblurring result from a single image of the moderate size in a few seconds in 2009. The related techniques could be used for other problems in image processing. Xu *et al.*[6] proposed an image smoothing method via L_0 gradient minimization in 2011, which can globally control the number of non-zero resulting in approximating prominent structures in a structure-sparsity-management way. Xu *et al.*[7] also proposed a new inherent variation and relative total variation (RTV) measure, which distinguishes the essential difference between these two types of visual forms: texture and structure. The new inherent variation can effectively extract the main structures, while RTV is not good enough for manipulating some small-scale details. Li *et al.*[8] proposed a hybrid domain edge-aware image processing method in 2013 which is able to synthesize a global optimization result. He *et al.*[9] proposed the guided filter in 2010, which uses a local linear model. Compared with BLF, guided filter not only preserves edges but also works much better in detail preservation. The time complexity of guided filter is independent of the size of the window and it is more efficient to process images when using large windows. Karacan *et al.*[10] proposed an alternative yet simple image smoothing approach which depends on covariance matrices of simple image features, a.k.a., the region covariances, in 2013. Min *et al.*[11] proposed a new method to optimize a fast global smoother with data items and smooth a priori in 2014. Zhang *et al.*[12] offered a new framework called rolling guided filter (RGF) to filter the images based on joint bilateral filter. It removes the texture by Gaussian filtering and then recovers the edge of the input image by BLF. But RGF may filter the non-texture component and cause ringing artifacts around edges. Bao *et al.*[13] proposed a tree filter in 2014, which is a trilateral filter. The tree filter removes the high contrast details by the minimum spanning tree. Bi *et al.*[14] introduced an image transform based on the L_1 norm for piecewise image flattening in 2015. Paris *et al.*[15] showed the state-of-the-art edge-aware processing using standard Laplacian pyramids in 2015. Their approach is simple and flexible. Zang *et al.*[16] developed a novel directional anisotropic structure measurement for adaptive image smoothing in 2015. Liu *et al.*[17] proposed a novel optimization model via the redundancy of natural images, by defining a nonlocal concentration regularization term on the gradient in 2015. This nonlocal constraint is carefully combined with a gradient-sparsity constraint, allowing details throughout the whole image to be removed automatically in a data-driven way. Zheng *et al.*[18] proposed a new learning-based weighted total variation (LTV) model in 2016, where the weights are learned from different kinds of texture images to well discriminate pixels belonging to structural contours from pixels belonging to texture.

However, image smoothing that removes the texture while preserving the main structure is a challenging problem. Most of the previous image smoothing methods cannot remove the texture obviously in many situations. In this paper, we propose a novel framework for image smoothing combined with the constraint of sparse high frequency component of texture images. The main contributions of our work are as follows. 1) We design a novel framework for image decomposition to deal with the high-frequency information of images with rich texture. 2) We show that the decomposed images can achieve obvious texture removal effects via sparse high-frequency gradient constraints. 3) An extensive experimental evaluation is presented by comparing the proposed method with some previous image smoothing approaches on natural images and high-texture images. Our experimental results show that the proposed method is much effective on texture removal.

The rest of the paper is organized as follows. In Section 2, we present the details of the proposed DSHFG (Decomposition and Sparse High Frequency Gradient) algorithm. Section 3 compares the proposed DSHFG algorithm with some previous image smoothing approaches and analyzes the result. In Section 4, we demonstrate the ability of our method in several applications. Finally, we conclude our work in Section 5.

2 Problem and Proposed Method

2.1 Problem

As aforementioned, the existing image smoothing methods are difficult to obtain significant texture removal performance in many situations, because the texture containing obvious edges and large gradient changes is easy to be preserved. As shown in Fig.1(b), smoothing the input image via L_0 gradient minimization[6] cannot get satisfactory results. We observe that the texture is mostly removed in the right dark area, but there are still a lot of texture patterns in the left area. The red channel is shown as it is representative of the main image content. In Fig.1(c),

the black curve represents the input signal and the red curve represents the smoothed signal via L_0 gradient minimization. The left dramatic changes in the input signal represent the texture component. The step in the middle of the input signal represents a main edge of the input image. The right of the input signal is the flat component. The red curve shows that L_0 smoothing regards the texture as the main edges and preserves some texture in the smoothed signal.

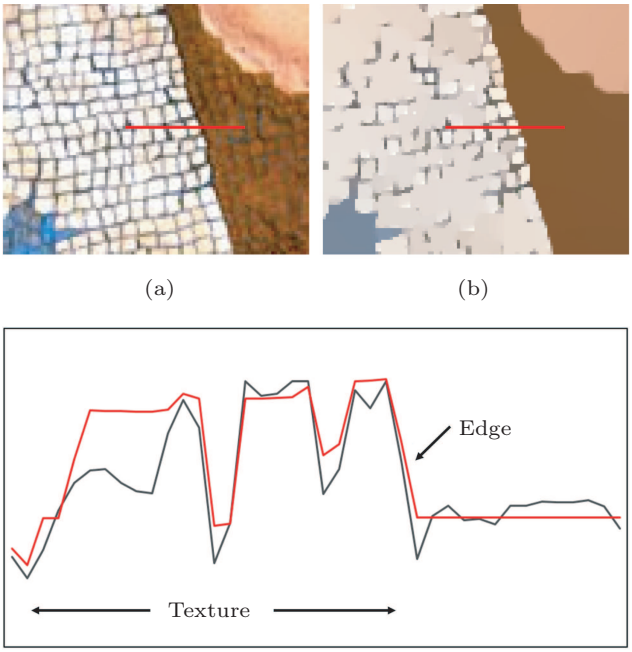

Fig.1. (a) Input image. (b) Smoothed image. (c) The black curve represents the input signal extracted from Fig.1(a) marked by red lines. The red curve represents the smoothed signal extracted from Fig.1(b) marked by red lines. Both curves use the red channel of the images because the red channel is representative of the main image content.

L_0 smoothing counts amplitude changes discretely in 1D signal, written as

$$c(f) = \#\{p \,|\, |f_p - f_{p+1}| \neq 0\}, \tag{1}$$

where p and $p+1$ index neighboring samples. $|f_p - f_{p+1}|$ is a gradient about p which is in the form of forward difference. $\#\{\cdot\}$ is the counting operator which counts the number of p that satisfies $|f_p - f_{p+1}| \neq 0$, that is, the L_0 norm of gradient. Because $c(f)$ does not count on gradient magnitude, $c(f)$ would not be affected if an edge only alters its contrast. Similar to TV[1], L_0 smoothing cannot get good texture removal results due to the effect of the high-frequency gradient of texture.

2.2 Idea of the Proposed Algorithm

In consideration of shortcomings of L_0 smoothing, in this paper, we present a novel framework for image decomposition to better apply the constraints for sparse high frequency gradients. First, we decompose the image into two components: a smooth component and a non-smooth component. Second we remove the non-smooth component containing high-frequency gradient and smooth the other component with the constraint of sparse high frequency gradient. Fig.2 shows the flowchart of the proposed DSHFG algorithm.

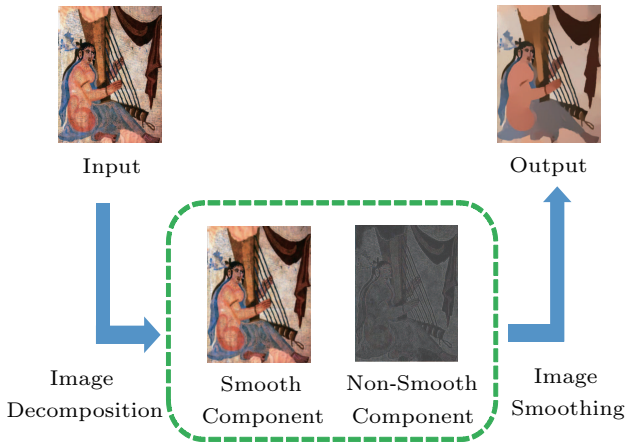

Fig.2. Flowchart of the proposed DSHFG algorithm.

2.2.1 *Image Decomposition*

Inspired by the image processing techniques[19-25] including image super-resolution techniques and image reconstruction techniques, we try to design a decomposition method to remove part of the high frequency information in texture images because the abundant high frequency information in texture images is not conducive to smoothing images directly. The general form used in most image processing methods based on optimization is to solve

$$\arg\min_u = \frac{1}{2}\|x-u\|_2^2 + \lambda\mathcal{R}(u).$$

In this formulation, x is the input image and u is the output image. The first term is to model data fidelity. $\mathcal{R}(u)$ is a regularization prior. λ is a parameter controlling the trade-off between data fidelity and the regularization of u. In the consideration of the abundant high frequency information in texture images, we use a low pass filter to filter out part of high frequency information. To keep the output image smooth at the same

time, the following formulation is designed:

$$\arg\min_{u} = \frac{1}{2}\|x - \Phi(u)\|_2^2 + \lambda\mathcal{R}(u),$$

where

$$\Phi(u) = f_L \otimes u,$$
$$\mathcal{R}(u) = \sum\nolimits_d \|g_d \otimes u\|_p.$$

In these formulations, f_L is a low pass filter of size 6×6, $\otimes$ is the convolution operator, and g_d is the gradient operator along multiple directions. $\mathcal{R}(u)$ enforces the output image u to be smooth. Fig.3 shows the low pass filter and the gradient operator along multiple directions.

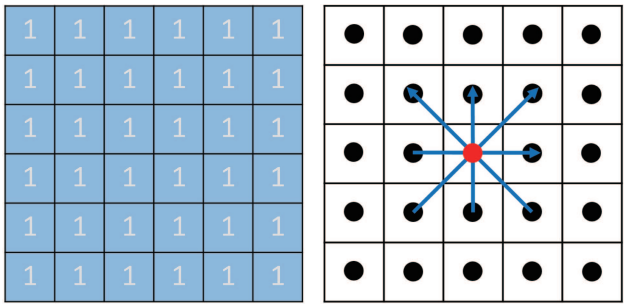

Fig.3. (a) Low pass filter of size 6×6. (b) Gradient operator along multiple directions.

Based on this idea, we propose the following method for image decomposition. It can obviously separate part of high frequency gradient from the input image and the high frequency gradient corresponds to the texture of the image. The key idea of our strategy is to decompose the input image into a smooth component x_L and a non-smooth component x_R. x_R contains much high-frequency information. In this work, we use the L_2 norm of $\mathcal{R}(u)$. The smooth component can be obtained by solving the following deconvolution problem:

$$x_L = \arg\min_{x_L} \frac{1}{2}\|x - f_L \otimes x_L\|_2^2 + k\sum_{d=1}^{4}\|g_d \otimes x_L\|_2^2,$$

where k is a manual setting parameter that affects the performance of image decomposition. We design g_d as the gradient operator along direction $d \in \{$ 1 = horizontal, 2 = vertical, 3 = 45 degrees, 4 = 135 degrees$\}$. We use the FFT (fast Fourier transform) operator $\mathcal{F}$ to solve this problem efficiently, i.e.,

$$x_L = \mathcal{F}^{-1}\left(\frac{\overline{\mathcal{F}(f_L)}\mathcal{F}(x)}{\overline{\mathcal{F}(f_L)}\mathcal{F}(f_L) + k\sum_d \overline{\mathcal{F}(g_d)}\mathcal{F}(g_d)}\right), \quad (2)$$

where $\overline{\bullet}$ is the complex conjugate operator. The plus, multiplication, and division are all component-wise operators. The residual component x_R is then obtained as

$$x_R = x - f_L \otimes x_L.$$

Fig.4 compares the gradient amplitude image of the input image with the gradient amplitude image of x_L after image decomposition, which shows that the gradient of x_L obtained in the texture segment is no longer violent.

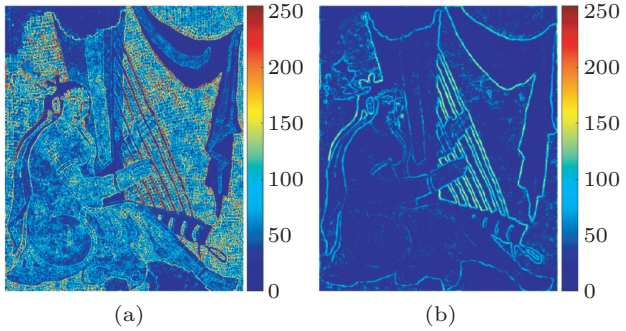

Fig.4. Visualized gradient amplitude map. Amplitudes are normalized to [0, 255] and colorized according to the colormap on the right. (a) Gradient map of the input image. (b) Gradient map of the smooth component x_L.

2.2.2 Constraint of Sparse High Frequency Gradient

After removing the non-smooth component containing high-frequency gradient, we need to smooth the other component with the constraint of sparse high frequency gradient. In the past, there were many methods to constrain the gradient of the image. The famous TV model constrains the gradient of the input image to preserve large-scale edges[1,26-28]. TV-L_2 model simply uses a quadratic penalty to enforce the structural similarity between the input and the output, expressed as

$$\arg\min_{S} \sum\nolimits_p \{\frac{1}{2\lambda}(S_p - I_p)^2 + |(\nabla S)_p|\},$$

where p indexes the pixel of the two-dimensional image. I is the input image, which could be the luminance (or log brightness) channel, and S is the resulting structure image. The data term $(S_p - I_p)^2$ is to make the structures in the output image similar to those in the input image. $\sum_p |(\nabla S)_p|$ is the total variation (TV) regularizer, written as

$$\sum\nolimits_p |(\nabla S)_p| = \sum\nolimits_p |(\partial x S)_p| + |(\partial y S)_p|.$$

This is an anisotropic expression in the two-dimensional image, and ∂x and ∂y are partial derivatives in two directions. We try to use the TV model to constrain x_L in

the previous image decomposition, but the experimental result shows that the TV model has limited ability to distinguish texture from strong structural edges. Therefore we use L_0 norm to constrain sparse high-frequency gradient[6], written as

$$\arg\min_{x_S} \|x_S - x_L\|_2^2 + \lambda \|\nabla x_S\|_0, \tag{3}$$

and the second term in (3) denotes the following formulation:

$$\|\nabla x_S\|_0 = \#\{p|\ |\nabla_x x_{S_p}| + |\nabla_y x_{S_p}| \neq 0\},$$

where x_L is the input image obtained from the image decomposition, x_S is the output image, ∇x_S is the gradient of x_S, and λ is the parameter to control the level of sparseness in the final output x_S. A larger λ produces a coarser result with less gradient. $\#\{\cdot\}$ denotes the number of the non-zero gradient pixels and p indexes the pixel of the image x_S. (1) shows the form in the dimensional signal. In the two-dimensional images, we use four-connected pixels of the p-th pixel.

However, the inclusion of the L_0 norm in the objective function makes it NP-hard. A splitting method that iteratively optimizes subproblems alternately[29] can be used as an effective technique. Both of the two subproblems find their closed-form solutions. We introduce two variables (h, v) corresponding to $(\nabla_x x_S, \nabla_y x_S)$ respectively, the new model can be represented as

$$\begin{aligned}&\arg\min_{x_S,h,v} \|x_S - x_L\|_2^2 + \lambda\|(h,v)\|_0 + \\ &\beta(\|h - \nabla_x x_S\|_2^2 + \|v - \nabla_y x_S\|_2^2),\end{aligned} \tag{4}$$

and the second term in (4) denotes the following formulation:

$$\|(h,v)\|_0 = \#\{p|\ |h_p| + |v_p| \neq 0\},$$

where β is an automatically adapting parameter to control the similarity between variables (h, v) and their corresponding gradients. (4) can be split into two subproblems which can be optimized iteratively. In each pass, one set of the variables are fixed with values obtained from the previous iteration.

Subproblem 1: *Computing* x_S. The following subproblem can be extracted from (4):

$$\arg\min_{x_S} \|x_S - x_L\|_2^2 + \beta(\|h - \nabla_x x_S\|_2^2 + \|v - \nabla_y x_S\|_2^2).$$

The solution is unique, but it is computationally complex to solve directly, requiring large matrix inversion. Thus, we use Gauss-Seidel iteration to solve it approximately and diagonalize derivative operators after FFT for speedup, written as

$$\begin{aligned}&x_S \\ &= \mathcal{F}^{-1}\left(\frac{\mathcal{F}(x_L) + \beta(\overline{\mathcal{F}(\nabla_x)}\mathcal{F}(h) + \overline{\mathcal{F}(\nabla_y)}\mathcal{F}(v))}{\mathcal{F}(1) + \beta(\overline{\mathcal{F}(\nabla_x)}\mathcal{F}(\nabla_x) + \overline{\mathcal{F}(\nabla_y)}\mathcal{F}(\nabla_y))}\right),\end{aligned} \tag{5}$$

where $\mathcal{F}$ is the FFT operator and $\overline{\bullet}$ is the complex conjugate operator. $\mathcal{F}(1)$ is the Fourier transform of the delta function. The plus, multiplication, and division are all component-wise operators.

Subproblem 2: *Computing* (h, v). The following subproblem can be extracted from (4):

$$\begin{aligned}&\arg\min_{h,v} \lambda\|(h,v)\|_0 + \beta(\|h - \nabla_x x_S\|_2^2 + \\ &\|v - \nabla_y x_S\|_2^2).\end{aligned} \tag{6}$$

For each pixel of x_S, we solve the following energy function, written as

$$\begin{aligned}E_p(h_p, v_p) =\ &\lambda\mathcal{H}(|h_p| + |v_p|) + \\ &\beta\left((h_p - \nabla_x x_{S_p})^2 + (v_p - \nabla_y x_{S_p})^2\right),\end{aligned}$$

where $\mathcal{H}(\cdot)$ represents the Heaviside function, i.e., $\mathcal{H}(t) = 1$ when $t \neq 0$ and $\mathcal{H}(t) = 0$ otherwise. The whole function in (6) is optimized when all subproblems E_p are solved. The solution is made tractable by using

$$(h_p, v_p) = \begin{cases}(0,0), & \text{if } (\nabla_x x_{S_p})^2 + (\nabla_y x_{S_p})^2 \leqslant \dfrac{\lambda}{\beta},\\ (\nabla_x x_{S_p}, \nabla_y x_{S_p}), & \text{otherwise.}\end{cases} \tag{7}$$

The whole procedure for image smoothing is summarized in Algorithm 1. In (2), f_L is a low pass filter of size 6×6. k is a manual setting parameter. In this

Algorithm 1 . Proposed DSHFG Algorithm

Input: original image x, parameter k, smoothing coefficient λ, parameter β_0, β_{MAX}, and rate n

1: Initialize: $k = 55$;
2: Compute image x_L using (2);
3: Initialize: $x_S^0 = x_L$, $\beta = \beta_0$, $i = 0$;
4: **while** $\beta < \beta_{\text{MAX}}$ **do**
5: Compute gradients (h_p^i, v_p^i) using (7);
6: Compute image x_S^{i+1} using (5);
7: $\beta = n\beta$, $i{+}{+}$;
8: **end while**
9: **return**

Output: smoothed image x_S

paper, k is 55 when smoothing the texture image. In (3), λ controls the smoothness. A larger λ produces greater smoothness with less gradient.

3 Comparison

In this section, we compare our method with a series of image smoothing methods. Firstly, there are two methods which can remove the texture relatively well. One is RTV[7] and the other is RGF[12]. The quality of the texture removal is mainly evaluated from two aspects: 1) whether the method can remove the texture as much as possible; 2) whether the method can preserve the main structure of the image. As shown in Fig.5, Fig.5(b) is the result of RTV. We observe that RTV removes most of the texture and does not blur the "face" in this image, but the details of "hair" are removed. Fig.5(c) shows the result of RGF. In this algorithm, the number of iterations is set to 12. RGF removes most of the texture as well, but the "hair" and the "eyes" are blurred and the details of "hair" and "eyes" are not clear enough. Fig.5(d) is the result of the proposed DSHFG algorithm. DSHFG removes the texture in the image as much as possible and preserves the main structure of the image at the same time. The "hair" and the "eyes" are not blurred and the details of them are not removed.

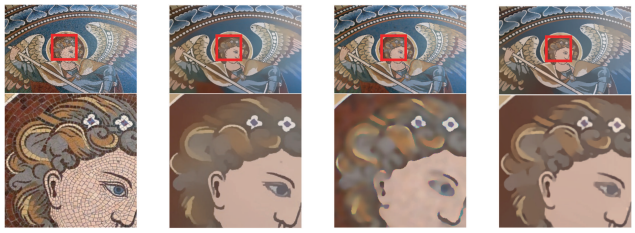

(a) (b) (c) (d)

Fig.5. Comparison of texture removal. (a) Original texture image. (b) Result of RTV ($\lambda = 0.03$, $\sigma = 2$). (c) Result of RGF ($\sigma_s = 5$, $\sigma_r = 0.1$, *iteration* $= 12$). (d) Result of the proposed DSHFG algorithm ($\lambda = 0.035$, $k = 55$).

Then Fig.6 shows the comparison of a series of image smoothing methods. As shown in Fig.6(b), the result of BLF[2] is not obvious. Fig.6(c) is the result of L_0 smoothing[6]. It shows that L_0 smoothing smoothes the image strongly, resulting in the loss of the details. Fig.6(d) shows the result of a fast global smoothing method based on weighted least squares (FGS)[11]. FGS does not work well in the flat areas and some edges. As shown in Fig.6(e), RGF smoothes better than BLF, but it still preserves some insignificant details which should be smoothed. In this algorithm, the number of iterations is set to 4. Fig.6(f) is result of the proposed DSHFG algorithm. The main objects are smoothed properly, and the insignificant details of the image are smoothed accurately. Compared with the methods mentioned above, the proposed DSHFG algorithm can get better visual quality of smoothing.

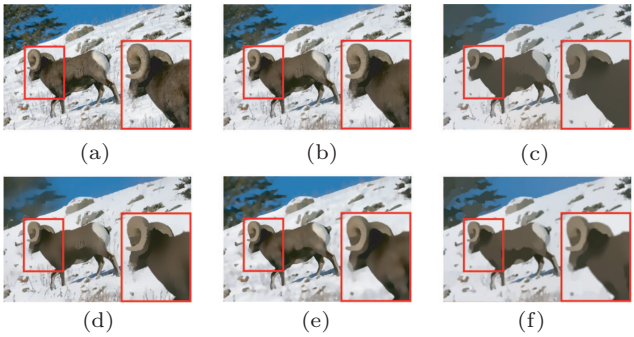

(a) (b) (c) (d) (e) (f)

Fig.6. Results of several smoothing methods. (a) Input image. (b) Result of BLF ($\sigma_r = 0.05$, $\sigma_s = 2$). (c) Result of L_0 ($\lambda = 0.05$). (d) Result of FGS ($\sigma = 0.03$). (e) Result of RGF ($\sigma_s = 4$, $\sigma_r = 0.15$, *iteration* $= 4$). (f) Result of the proposed DSHFG algorithm ($\lambda = 0.02$, $k = 30$).

4 Applications

There are many applications of image smoothing in image processing. We apply the proposed DSHFG algorithm to edge detection, detail magnification and image abstraction. Besides, DSHFG can be applied to image composition. The input image is pre-proposed by the proposed image smoothing algorithm, and a principal structure image is achieved. Then the principal structure image is fused with a background image to get a new image.

4.1 Edge Detection and Operation

Edge Detection. There are rich details such as texture in natural images which can influence the performance of edge detection. DSHFG can remove trivial details and preserve principle edges. As illustrated in Fig.7, many fine edges are included in the original gradient map. When we detect edges in the input image, there are many slight edges in the edge map. Then we produce a gradient map on our smoothed result. The gradient map mainly contains meaningful edges and the edge map detected on our smoothed image by the Canny operator contains fewer slight edges and is much clearer.

Image Abstraction. Image abstraction is applied in many image editing tools. It gives the developing demand for image editing tools for amateur users[30]. Our

method can serve as the abstracting tool. An example of image abstraction using our method is illustrated in Fig.8. First, we smooth the input image, and then edges are detected in the smooth image. Finally, the extracted edge map is enhanced and added back to augment the visual distinctiveness of different regions.

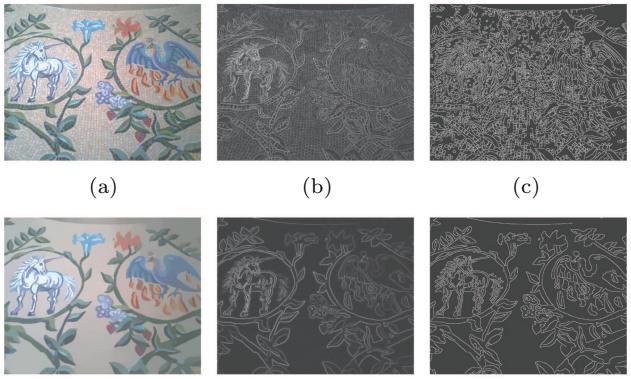

Fig.7. Edge detection. (a) Input image. (b) Gradient map of (a). (c) Edge map of (a). (d) Smoothed image. (e) Gradient map of (d). (e) Edge map of (d).

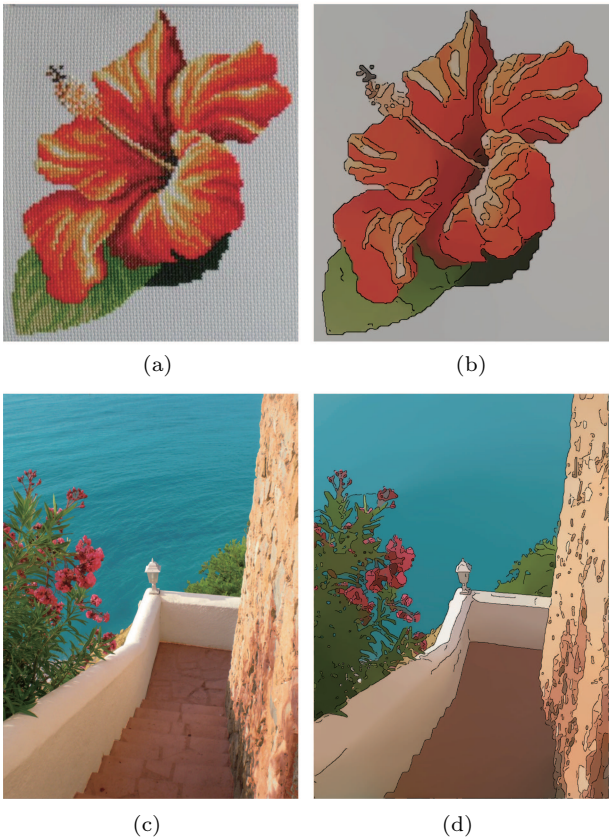

Fig.8. Image abstraction. (a) Texture image. (b) Result of (a). (c) Natural image. (d) Result of (c).

4.2 Detail Magnification

When the details of an image are not obvious enough, we can enhance the details of the original image with a simple detail magnification method. First, for the given image, we get a smooth layer and a detail layer using our image smoothing method. Then we enhance gradients in the detail layer, e.g., using a difference of Gaussian (DoG) operator. Finally, the enhanced detail layer is composed with the smooth layer. Fig.9 shows the input images and their magnification results.

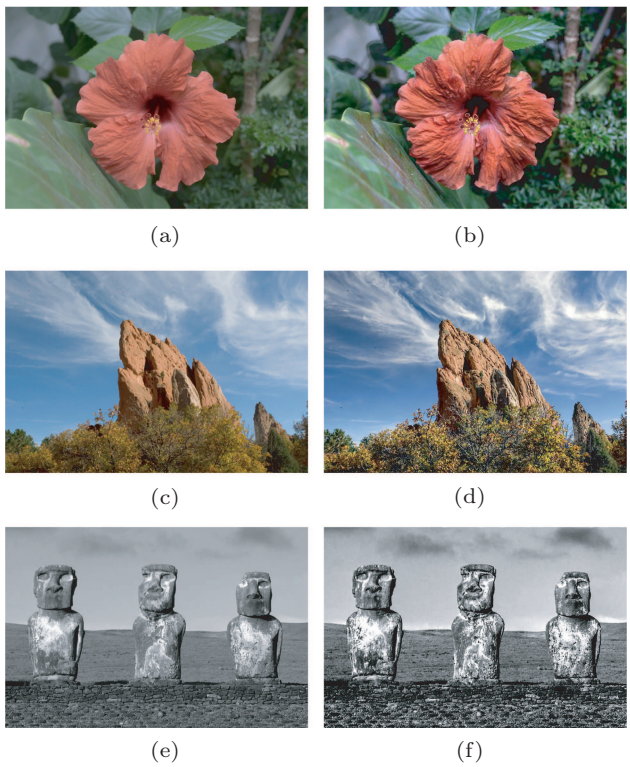

Fig.9. Detail magnification. (a) Flower. (b) Result of (a). (c) Hill. (d) Result of (c). (e) Stone. (f) Result of (e).

4.3 Image Composition

The drawings, paintings, and graffiti images usually cannot be directly used in image composition[31], because the structure of the target and source images do not match. Therefore we extract the principle structure such as words and patterns from the source image by the proposed DSHFG algorithm and then merge the structure image and the target image. As shown in Fig.10, the composition is much more natural using our produced structure images.

(a) (b)

(c) (d)

Fig.10. Image composition. (a) Input image. (b) Smoothed image. (c) Result of (a). (d) Result of (b).

5 Conclusions

A novel framework for image smoothing was proposed based on image decomposition and the sparse high frequency component of images. Experiments on both nature images and images with rich texture such as drawings, paintings, and graffiti images demonstrated that the proposed DSHFG algorithm achieves much better performance. Furthermore, DSHFG can be flexibly embedded into various image processing applications. In future work, we will try to combine our DSHFG algorithm and machine learning to speed up our algorithm and improve the texture removal performance.

References

[1] Rudin L I, Osher S, Fatemi E. Nonlinear total variation based noise removal algorithms. *Physica D: Nonlinear Phenomena*, 1992, 60(1/2/3/4): 259-268.

[2] Tomasi C, Manduchi R. Bilateral filtering for gray and color images. In *Proc. the 6th IEEE Int. Conf. Computer Vision*, January 1998, pp.839-846.

[3] Farbman Z, Fattal R, Lischinski D, Szeliski R. Edge-preserving decompositions for multi-scale tone and detail manipulation. *ACM Trans. Graphics*, 2008, 27(3): Article No. 67.

[4] Subr K, Soler C, Durand F. Edge-preserving multiscale image decomposition based on local extrema. *ACM Trans. Graphics*, 2009, 28(5): Article No. 147.

[5] Cho S, Lee S. Fast motion deblurring. *ACM Trans. Graphics*, 2009, 28(5): Article No. 145.

[6] Xu L, Lu C W, Xu Y, Jia J Y. Image smoothing via L_0 gradient minimization. *ACM Trans. Graphics*, 2011, 30(6): Article No. 174.

[7] Xu L, Yan Q, Xia Y, Jia J Y. Structure extraction from texture via relative total variation. *ACM Trans. Graphics*, 2012, 31(6): Article No. 139.

[8] Li X Y, Gu Y, Hu S M, Martin R R. Mixed-domain edge-aware image manipulation. *IEEE Trans. Image Processing*, 2013, 22(5): 1915-1925.

[9] He K M, Sun J, Tang X O. Guided image filtering. *IEEE Trans. Pattern Analysis and Machine Intelligence*, 2013, 35(6): 1397-1409.

[10] Karacan L, Erdem E, Erdem A. Structure-preserving image smoothing via region covariances. *ACM Trans. Graphics*, 2013, 32(6): Article No. 176.

[11] Min D B, Choi S, Lu J B, Ham B, Sohn K, Do M N. Fast global image smoothing based on weighted least squares. *IEEE Trans. Image Processing*, 2014, 23(12): 5638-5653.

[12] Zhang Q, Shen X Y, Xu L, Jia J Y. Rolling guidance filter. In *Proc. the 13th European Conf. Computer Vision*, September 2014, pp.815-830.

[13] Bao L C, Song Y B, Yang Q X, Yuan H, Wang G. Tree filtering: Efficient structure-preserving smoothing with a minimum spanning tree. *IEEE Trans. Image Processing*, 2014, 23(2): 555-569.

[14] Bi S, Han X G, Yu Y Z. An L_1 image transform for edge-preserving smoothing and scene-level intrinsic decomposition. *ACM Trans. Graphics*, 2015, 34(4): Article No. 78.

[15] Paris S, Hasinoff S W, Kautz J. Local Laplacian filters: Edge-aware image processing with a Laplacian pyramid. *Communications of the ACM*, 2015, 58(3): 81-91.

[16] Zang Y, Huang H, Zhang L. Guided adaptive image smoothing via directional anisotropic structure measurement. *IEEE Trans. Visualization and Computer Graphics*, 2015, 21(9): 1015-1027.

[17] Liu Q, Zhang C M, Guo Q, Zhou Y F. A nonlocal gradient concentration method for image smoothing. *Computational Visual Media*, 2015, 1(3): 197-209.

[18] Zheng S F, Song C W, Zhang H Z, Yan Z F, Zuo W M. Learning-based weighted total variation for structure preserving texture removal. In *Proc. Chinese Conf. Pattern Recognition*, November 2016, pp.147-160.

[19] Gu S H, Zuo W M, Xie Q, Meng D Y, Feng X C, Zhang L. Convolutional sparse coding for image super-resolution. In *Proc. IEEE Int. Conf. Computer Vision*, December 2015, pp.1823-1831.

[20] Zhang M L, Desrosiers C. Image completion with global structure and weighted nuclear norm regularization. In *Proc. IEEE Int. Joint Conf. Neural Networks*, May 2017, pp.4187-4193.

[21] Lu S P, Dauphin G, Lafruit G, Munteanu A. Color retargeting: Interactive time-varying color image composition from time-lapse sequences. *Computational Visual Media*, 2015, 1(4): 321-330.

[22] Wu L Q, Liu Y P, Brekhna, Liu N, Zhang C M. High-resolution images based on directional fusion of gradient. *Computational Visual Media*, 2016, 2(1): 31-43.

[23] Li Q H, Fang Y M, Xu J T. A novel spatial pooling strategy for image quality assessment. *Journal of Computer Science and Technology*, 2016, 31(2): 225-234.

[24] Xie H, Tong R. Patch-based variational image approximation. *Science China Information Sciences*, 2017, 60(3): 032104.

[25] Du H W, Zhang Y F, Bao F X, Wang P, Zhang C M. A texture feature preserving image interpolation algorithm via gradient constraint. *Communications in Information and Systems*, 2016, 16(4): 203-227.

[26] Meyer Y. Oscillating Patterns in Image Processing and Nonlinear Evolution Equations: The Fifteenth Dean Jacqueline B. Lewis Memorial Lectures. American Mathematical Society, 2001.

[27] Yin W T, Goldfarb D, Osher S. Image cartoon-texture decomposition and feature selection using the total variation regularized L^1 functional. In *Proc. Variational Geometric and Level Set Methods in Computer Vision*, October 2005, pp.73-84.

[28] Aujol J F, Gilboa G, Chan T, Osher S. Structure-texture image decomposition-modeling, algorithms, and parameter selection. *International Journal of Computer Vision*, 2006, 67(1): 111-136.

[29] Wang Y L, Yang J T, Yin W T, Zhang Y. A new alternating minimization algorithm for total variation image reconstruction. *SIAM Journal on Imaging Sciences*, 2008, 1(3): 248-272.

[30] Zhang S H, Li X Y, Hu S M, Martin R R. Online video stream abstraction and stylization. *IEEE Trans. Multimedia*, 2011, 13(6): 1286-1294.

[31] Pérez P, Gangnet M, Blake A. Poisson image editing. *ACM Trans. Graphics*, 2003, 22(3): 313-318.

Guang-Hao Ma is currently a M.S. student in the School of Computer Science and Technology, Shandong University, Jinan. He received his B.S. degree in computer science from Shandong University, Weihai, in 2015. His research interests include image smoothing and computer vision.

Ming-Li Zhang received her Ph.D. degree in image processing from école de Technologie Supérieure, University of Quebec, Montreal, in 2017. Her research focuses on designing and application of high-performance machine learning models to solve problems in the fields of computer vision, biomedical imaging and natural images. She is a scientist in Shandong Co-Innovation Center of Future Intelligent Computing, Yantai. She is now a postdoctoral research fellow in Mcgill Centre for Integrative Neuroscience/Ludmer Centre for NeuroInformatics and Mental Health, Montreal Neurological Institute, Mcgill University, working on brain image analysis.

Xue-Mei Li received her Master's and Ph.D. degrees in computer science and technology from Shandong University, Jinan, in 2004 and 2010, respectively. She is currently an associate professor in School of Software, Shandong University, Jinan, and a member of the Geometric Design and Information Visualization (GD & IV) Laboratory, Shandong University, Jinan. She is engaged in research on geometric modeling, computer aided geometric design, medical image processing and information visualization.

Cai-Ming Zhang is a professor and doctoral supervisor of the School of Software at Shandong University, Jinan. He is now also the dean of the Digital Media Research Institute at Shandong University of Finance and Economics, Jinan. He received his B.S. and M.S. degrees in computer science from Shandong University, Jinan, in 1982 and 1984, respectively, and his Ph.D. degree in computer science from the Tokyo Institute of Technology, Tokyo, in 1994. From 1997 to 2000, Dr. Zhang had held visiting position at the University of Kentucky, Lexington. His research interests include computer aided geometric design, computer graphics, information visualization, and medical image processing.